

Molecular Pathogenesis of Genetic and Inherited Diseases

# Matrix Metalloproteinase Inhibitor Batimastat Alleviates Pathology and Improves Skeletal Muscle Function in Dystrophin-Deficient *mdx* Mice

Akhilesh Kumar, Shephali Bhatnagar,  
and Ashok Kumar

From the Department of Anatomical Sciences and Neurobiology,  
University of Louisville School of Medicine, Louisville, Kentucky

**Duchenne muscular dystrophy (DMD), caused by mutations in the dystrophin gene, involves severe muscle degeneration, inflammation, fibrosis, and early death in afflicted boys. Matrix metalloproteinases (MMPs) are extracellular proteases that cause tissue degradation in several disease states. In this study, we tested the hypothesis that the expression levels of various MMPs are abnormally increased and that their inhibition will ameliorate muscle pathogenesis in animal models of DMD. Our results show that the transcript levels of several MMPs are significantly up-regulated, whereas tissue inhibitors of MMPs are down-regulated, in dystrophic muscle of *mdx* mice. Chronic administration of batimastat (BB-94), a broad spectrum peptide inhibitor of MMPs, reduced necrosis, infiltration of macrophages, centronucleated fibers, and the expression of embryonic myosin heavy chain in skeletal muscle of *mdx* mice. Batimastat also reduced the expression of several inflammatory molecules and augmented the levels of sarcolemmal protein  $\beta$ -dystroglycan and neuronal nitric oxide in *mdx* mice. In addition, muscle force production in isometric contraction was increased in batimastat-treated *mdx* mice compared with those treated with vehicle alone. Furthermore, inhibition of MMPs using batimastat reduced the activation of mitogen-activated protein kinases and activator protein-1 in myofibers of *mdx* mice. Our study provides the novel evidence that the expression of MMPs is atypically increased in DMD, that their inhibition ameliorates pathogenesis, and that batimastat could prove to be a significant candidate for DMD therapy. (Am J Pathol 2010, 177:248–260; DOI: 10.2353/ajpath.2010.091176)**

or partial deficiency of dystrophin.<sup>1,2</sup> Dystrophin is an integral component of the transmembrane protein network known as dystrophin-glycoprotein complex (DGC) in sarcolemma, which not only provides mechanical stability but also serves as an important signaling link between extracellular matrix stimuli and intracellular components of skeletal muscle.<sup>3,4</sup> Loss of functional dystrophin protein makes sarcolemma fragile, resulting in ready damage during muscle contraction leading to the initiation of inflammatory response, degradation of the components of cytoskeletal-extracellular matrix (ECM) network, and fiber necrosis.<sup>5</sup> Lack of dystrophin protein on sarcolemma also results in the aberrant activation of many proinflammatory signal transduction pathways in skeletal muscle, which contributes to pathogenesis.<sup>4,6–8</sup> However, despite major progress in understanding the pathophysiological mechanisms, there is still no therapy available for DMD patients.

Studies in the recent past have demonstrated that secondary events such as inflammation, cycles of fiber degeneration and regeneration, and fibrosis contribute actively to skeletal muscle pathogenesis in DMD.<sup>6,7,9,10</sup> Matrix metalloproteinases (MMPs) are a family of zinc-dependent endopeptidases that play an important role in ECM degradation, inflammation, fibrosis, and activation of latent cytokines and cell adhesion molecules in different pathophysiological conditions.<sup>11</sup> MMPs are synthesized as secreted or transmembrane proenzymes and then processed to an active enzyme by the removal of an amino-terminal propeptide.<sup>11,12</sup> Abnormal increase in MMP levels has been found to contribute to tissue destruction in many pathological conditions such as chronic wounds, heart failure, rheumatic arthritis, fibrotic lung disease, dilated cardiomyopathy, asthma, gastric ulcer, central nervous system diseases, multiple sclerosis, and

Supported in part by Institutional Start-Up Funds and a National Institutes of Health grant R01 AG129623 (A.K.).

Accepted for publication March 12, 2010.

Address reprint requests to Ashok Kumar, Ph.D., Associate Professor, Department of Anatomical Sciences and Neurobiology, University of Louisville School of Medicine, 500 South Preston Street, Louisville, KY 40202. E-mail: ashok.kumar@louisville.edu.

Duchenne muscular dystrophy (DMD) is a devastating genetic disorder of skeletal muscle caused by complete

cancer.<sup>11,13–17</sup> Recent studies using transgenic and knockout mouse models have further revealed that MMPs also play critical roles in various physiological processes such as development, cell migration, and release of growth factors during tissue repair, as well as participate in host protective mechanisms.<sup>11,12</sup> Furthermore, the role of individual MMPs has been found to be dependent on stages of disease progression, suggesting that MMP inhibition can have both advantageous and disadvantageous consequences.<sup>18,19</sup> The contribution of MMPs in physiological processes has also been highlighted by the observations that several broad-spectrum MMP inhibitory drugs failed in multiple clinical trials for various types of cancer.<sup>19</sup> However, the potential role of MMPs in skeletal muscle loss and whether the inhibition of MMPs can be used as therapeutic option in muscular dystrophy patients are not yet investigated.

We recently reported that the expression of MMP-9 (gelatinase B) is increased in dystrophic muscle and genetic ablation of MMP-9 considerably reduces inflammatory response, fibrosis, and enhances the regeneration of myofibers in *mdx* mice (a murine model of DMD).<sup>20</sup> However, accumulating evidence also suggests that there is a cooperative interaction between various MMPs to regulate tissue degradation in different physiological and pathophysiological conditions. The members of the MMPs family often activate each other, for example, membrane type 1 metalloproteinase (MT1-MMP) activates MMP-2 or MMP-13 and MMP-3 activates MMP-9.<sup>11,12,21</sup> However, it remains unknown how the levels and the activities of various MMPs other than MMP-9 are regulated in skeletal muscle of *mdx* mice. Furthermore, it remains unknown whether MMP inhibitory molecules can improve skeletal muscle pathology in animal models of DMD.

Because MMPs are strongly linked to tissue degradation in several disease states, in the past decade, a number of pharmacological compounds/drugs have been developed that can block the activity of a specific or multiple MMPs in animal models and humans.<sup>18</sup> Batimastat (BB-94) and its orally bioavailable derivative marimastat, are collagen peptide-based hydroxamic acids. These were among the first synthetic MMP inhibitors evaluated to treat cancer.<sup>18,19</sup> Batimastat mimics the site in the collagen substrate that is cleaved by the MMPs and works by a competitive, reversible inhibition.<sup>22,23</sup> It is one of the most important broad-spectrum MMP inhibitors, effectively blocking the activities of MMP-1 (MMP-13 in rats), MMP-2, MMP-3, MMP-7, MMP-8, MMP-9, and MMP-14.<sup>22–24</sup> Batimastat and marimastat have been reported to inhibit growth, invasion, and metastasis as well as to prolong survival in rodent cancer models.<sup>23,25–28</sup> While batimastat and marimastat were found to show beneficial effects in Phase II and III trials in some type of cancer patients, so far no clinical trial has been considered as successful because of deleterious side effects.<sup>19,29–34</sup> However, it is noteworthy that cancer is a highly complex disorder involving multiple factors. Furthermore, all of the clinical trials using MMP inhibitors were performed in advanced stage cancer patients where the inhibition of MMPs might not be sufficient to block growth and spread of malignant cells.<sup>19</sup> In contrast to cancer, DMD, a genetic disorder

caused due to mutations in a single gene (ie, dystrophin), can be detected at an early stage, progresses in a much milder fashion, and can be treated before the pathology is fully established.

To understand the role of MMPs in the DMD, in this study, we first investigated how the expression of various MMPs and related molecules involved in ECM remodeling is affected in skeletal muscle of *mdx* mice. We have also investigated the effects of chronic administration of batimastat on skeletal muscle pathology and function in *mdx* mice.

## Materials and Methods

### Animals and Treatment Protocol

Control (strain C57BL10/ScSn) and *mdx* (strain C57BL10ScSn DMD<sup>*mdx*</sup>) mice were purchased from Jackson Laboratory (Bar Harbor, ME). Control and *mdx* mice were treated with batimastat (BB-94) using a protocol as described.<sup>35</sup> Starting at the age of 2 weeks, control and *mdx* mice were given intraperitoneal injections of batimastat (30 mg/kg as a suspension of 3 mg/ml in phosphate-buffered saline containing 0.01% Tween 80) three times a week for a total of 5 weeks. Batimastat untreated mice received the same volume of vehicle alone. After 24 hours of final administration of batimastat, the mice were sacrificed and skeletal muscles were isolated and analyzed. All experiments with animals were approved by the Institutional Animal Care and Use Committee of the University of Louisville.

### PCR Array Analysis

RNeasy Mini Kit (Qiagen) was used to extract total RNA from skeletal muscle tissues<sup>36</sup> and contaminating DNA was removed using the DNA-free kit from Ambion (Austin, TX). Quality and quantity of RNA were analyzed using an Agilent 2100 Bioanalyzer (Agilent, Palo Alto, CA) and NanoDrop instrumentation (NanoDrop Technologies, Wilmington, DE). Purified RNA (1  $\mu$ g) was used to synthesize first strand cDNA by reverse transcription system using Ambion's oligo(dT) primer and Qiagen's Omniscript reverse transcriptase according to the manufacturer's instructions. For the PCR array experiments, an RT<sup>2</sup> Profiler PCR Array (SABiosciences, Frederick, MD) was used to simultaneously examine the mRNA levels of 89 genes, including five housekeeping genes, in 96-well plates according to the manufacturer's protocol. Equal amounts of cDNA made from gastrocnemius muscle from four control or four *mdx* mice were pooled. Real-time PCR was performed using an ABI Prism 7300 sequence detection system (Applied Biosystems, Foster City, CA). Data analysis and fold change in gene expression values were calculated using online software provided by the manufacturer (SABiosciences, Frederick, MD).

### Quantitative Real-Time PCR (QRT-PCR)

Real-time PCR for individual genes was performed using an ABI Prism 7300 sequence detection system (Applied Biosystems) using a method as previously described.<sup>36,37</sup> Briefly, the first-strand cDNA reaction (0.5  $\mu$ l) from gastrocnemius muscle of individual control or *mdx* mice ( $n = 4$  in each group) was subjected to real-time PCR amplification using gene-specific primers. The primers were designed according to ABI primer express instructions using Vector NTI software and were purchased from Sigma-Genosys (Spring, TX). The sequences of the primers used are as follows: MMP-3: 5'-GTGTGTGGTTGTGTGCTCATCCTA-3' (forward) and 5'-CCCAGGAACTTCTGCATTCT-3' (reverse); MMP-10: 5'-GCATTCAATCCCTGTATGGAGC-3' (forward) and 5'-TTCAGGCTCGGGATTCCAAT-3' (reverse); MMP-14: 5'-ATTTGCTGAGGGTTCCACG-3' (forward) and 5'-TCGGCAGAATCAAAGTGGGT-3' (reverse); ICAM-1: 5'-GGTGGTGAAGTCTGTCAAACAGGA-3' (forward) and 5'-AACATAAGAGGCTGCCATCACG-3' (reverse); VCAM-1: 5'-TCTATTTCACTCACACCAGCCCG-3' (forward) and 5'-ATCCAAAGTACCGTTGAGGCTCC-3' (reverse); Col1a1: 5'-TCAAGATGGTCGCGCTGGAC-3' (forward) and 5'-CCTTTCCAGTTCTCCAGCG-3' (reverse); Col3a1: 5'-GTGAACGTGGCTCTAATGGCAT-3' (forward) and 5'-AATAGGACCTGGATGCCACTT-3' (reverse); TIMP-2: 5'-GTGACTTCATTGTGCCCTGGG-3' (forward) and 5'-TGGGACAGCGAGTGATCTTGC-3' (reverse); TIMP-3: 5'-CAGATGAAGATGTACCGAGGCTTC-3' (forward) and 5'-AACCCAGGTGGTAGCGTAATT-3' (reverse); CD68: 5'-TACTCTCCTGCCATCCTCACGA-3' (forward), and 5'-CCATTTGTGGTGGGAGAACTGTG-3' (reverse); Mac-1: 5'-AGGGTTGTCCAGCCGATGATAT-3' (forward), and 5'-CCCAGCTTCTTGACGTTGTTGA-3' (reverse); TNF- $\alpha$ : 5'-GCATGATCCGCGACGTGGAA-3' (forward) and 5'-AGATCCATGCCGTTGGCCAG-3' (reverse); Myogenin: 5'-CATCCAGTACATTGAGCGCCTA-3' (forward) and 5'-GAGCAAATGATCTCCTGGGTTG-3' (reverse);  $\beta$ -actin, 5'-CAGGCATTGCTGACGGATG-3' (forward) and 5'-TGCTGATCCACATCTGCTGG-3' (reverse); and MYH4 5'-GGAACAGTATGAAGAGGAGCAGGA-3' (forward), and 5'-ATTCTGAAGTCGCTGCTTCGTC-3' (reverse).

Real-time PCR assays were performed in approximately 25- $\mu$ l reactions, consisting of 2X (12.5  $\mu$ l) Brilliant SYBR Green QPCR Master Mix (Stratagene), 400 nmol/L primers (0.5  $\mu$ l each from the stock), 11  $\mu$ l of water, and 0.5  $\mu$ l of template. The thermal conditions consisted of an initial denaturation at 95°C for 10 minutes followed by 40 cycles of denaturation at 95°C for 15 seconds, annealing and extension at 60°C for 1 minute, and, for a final step, a melting curve of 95°C for 15 seconds, 60°C for 15 seconds, and 95°C for 15 seconds. All reactions were performed in triplicate to reduce variation. The data were analyzed using SDS software version 2.0, and the results were exported to Microsoft Excel for further analysis. Data normalization was accomplished using two endogenous control ( $\beta$ -actin) and myosin heavy chain 4 (MyHC4), and the normalized values were subjected to a  $2^{-\Delta\Delta Ct}$  formula to calculate the fold change between the control and experimental groups. The formula and its

derivations were obtained from the ABI Prism 7900 sequence detection system user guide.

### Western Blotting

Quantitative estimation of specific protein was done by Western blot using a method as previously described.<sup>36</sup> Briefly, skeletal muscle tissues were washed with PBS and homogenized in lysis buffer A [50 mmol/L Tris-Cl (pH 8.0), 200 mmol/L NaCl, 50 mmol/L NaF, 1 mmol/L dithiothreitol, 1 mmol/L sodium orthovanadate, 0.3% IGEPAL, and protease inhibitors]. Approximately 100  $\mu$ g of protein was resolved on each lane on 8–12% SDS-polyacrylamide gel electrophoresis, electrotransferred onto nitrocellulose membrane and probed using anti- $\beta$ -dystroglycan (1:500, Santa Cruz), anti-embryonic myosin heavy chain (E-MyHC) (1:100, Developmental Studies Hybridoma Bank), anti-utrophin (1:100; Developmental Studies Hybridoma Bank), anti- $\alpha$ -dystroglycan (Santa Cruz), anti- $\alpha$ -dystrobrevin (1:500; Santa Cruz), anti-neuronal nitric oxide synthase (nNOS) (1:500; Santa Cruz), anti-phospho-p44/p42 (1:1000, Cell Signaling), anti-phospho-JNK1/2 (1:1000, Cell signaling, Inc), anti-phospho-p38 (1:500, Santa Cruz), anti-total p44/p42 (1:1000, Cell Signaling, Inc), anti-total JNK1/2 (1:1000, Santa Cruz), anti-total p38 (1:1000, Cell Signaling, Inc.), and anti- $\alpha$ -tubulin (1:2000, Cell Signaling, Inc.) and detected by chemiluminescence.

### MMP Assays

Fold difference in MMPs enzymatic activity was determined using the Sensolyte 520 Generic MMP Assay Kit, which measures the activity of a variety of MMPs, including MMP-1, 2, 3, 7, 8, 9, 12, 13, and 14 (AnaSpec, Fremont, CA). Briefly, skeletal muscle extracts were prepared in lysis buffer A and 100  $\mu$ g protein lysates were incubated with the FAM/QXL 520 fluorescence resonance energy transfer substrate for 1 hour in a black 96-well plate at room temperature in the dark. Measurements were made using SpectraMax M5 microplate reader (excitation at 490 nm, emission at 520 nm).

### Electrophoretic Mobility Shift Assay

The DNA binding activity of the AP-1 transcription factor was measured using electrophoretic mobility shift assay as detailed previously.<sup>4</sup> Briefly, 25  $\mu$ g of nuclear extract prepared from skeletal muscle was incubated with 16 fmol [<sup>32</sup>P] $\gamma$ -ATP end-labeled AP-1 consensus double-stranded oligonucleotide (Promega, MA) for 20 minutes at 37°C. The incubation mixture included 2 to 3  $\mu$ g of poly dI.dC in a binding buffer (25 mmol/L HEPES, pH 7.9, 0.5 mmol/L EDTA, 0.5 mmol/L dithiothreitol, 1% IGEPAL, 5% glycerol, 50 mmol/L NaCl). The DNA-protein complex thus formed was separated from free oligonucleotides on a 7.5% native polyacrylamide gel. The gel was dried, and radioactive bands were visualized and quantitated by PhosphorImager using ImageQuant TL software (GE Health care, Piscataway, NJ).

### *Histomorphometric and Immunofluorescence Studies*

Serial cross-sections (10  $\mu\text{m}$  thick) from mid-belly of frozen skeletal muscle tissues were mounted on glass slides and stained for H&E using standard protocol.<sup>20</sup> Pictures of the whole muscle sections were captured and the percentage of centrally nucleated fibers was counted in the entire muscle section. To quantify the variation in fiber size, fiber cross-sectional area was measured for every fiber in each section using Nikon NIS Elements BR 3.00 software (Nikon). Variability in cross-sectional areas between samples was expressed as the mean of the standard deviations for each population. The extent of fibrosis in muscle cryosections was determined using a Sirius red dye staining kit following a protocol suggested by manufacturer (American Master Tech).

For immunofluorescence staining, muscle sections were fixed in acetone for 10 minutes and air dried. The sections were blocked in 1% bovine serum albumin in PBS for 1 hour, and incubated with primary antibody in blocking solution at 4°C overnight under humidified conditions. The sections were washed three times with PBS before incubation with secondary antibody for 1 hour at room temperature and then washed three times for 30 minutes each with PBS. The slides were mounted using fluorescence medium with DAPI (Vector Laboratories), visualized under a fluorescent microscope (Nikon) and images were captured using Nikon DS Fi1 camera (Nikon). The dilution and source of primary antibodies are as follows: Anti-Mac-1 (1:100, Developmental Studies Hybridoma Bank, University of Iowa, Iowa City, IA), anti-laminin (1:100, Sigma), and anti-E-MyHC (1:50, Developmental Studies Hybridoma Bank, University of Iowa). Alexa Fluor 488 or Alexa Fluor 596-conjugated secondary antibodies were obtained from Invitrogen and used at 1:3000 dilutions.

To study the effects of batimastat on sarcolemmal permeability and fiber necrosis, muscle sections were stained with Cy3-labeled goat anti-mouse IgG (Invitrogen) and the number of IgG-filled fibers in two different sections of each gastrocnemius muscle (two muscles from each mouse) was counted as described.<sup>20</sup> Data are presented as average number of permeable/damaged fibers per muscle section.

### *Skeletal Muscle Functional Studies*

The force production in isometric contractions was measured using a similar method as described.<sup>20</sup> After anesthetizing the mice, intact diaphragm was isolated and immediately placed into a muscle bath with continuously circulating oxygenated 95% O<sub>2</sub>-5% CO<sub>2</sub> Krebs-Ringer solution (in mmol/L: 135 NaCl, 5 KCl, 2.5 CaCl<sub>2</sub>, 1 MgSO<sub>4</sub>, 1 NaH<sub>2</sub>PO<sub>4</sub>, 15 NaHCO<sub>3</sub> and 11 glucose). A muscle strip (2 mm in width) from the costal region of the diaphragm was excised under a stereomicroscope and transferred to 37°C oxygenated Krebs-Ringer solution for equilibration for 15 minutes before contractile studies. The muscle was mounted between a Fort25 force transducer (World

Precision Instrumentation) and a micromanipulator device in a temperature-controlled myobath (World Precision Instrumentation). The muscle was positioned between platinum wire stimulating electrodes and stimulated to contract isometrically using electrical field stimulation (supramaximal voltage, 1.2 ms pulse duration) using a Grass S88 stimulator. In each experiment, muscle length was adjusted to optimize twitch force (optimal length,  $L_o$ ). The output of the force transducer was recorded in computer using LAB-TRAX-4 software. To investigate a potentially different frequency response between groups, titanic contractions were assessed by sequential stimulation at 25, 50, 75, 100, 150, 200, and 300 Hz with 2 minutes of rest in between. The cross-sectional area for each muscle was determined by dividing muscle weight by its length and tissue density (1.06 g/L), and muscle force was compared after correction for cross-sectional area.

### *Statistical Significance*

Results are expressed as mean  $\pm$  SD. Statistical analysis used Student's *t*-test to compare quantitative data populations with normal distribution and equal variance. A value of  $P < 0.05$  was considered statistically significant unless otherwise specified.

## **Results**

### *Expressions and Activities of Various MMPs Are Increased in Skeletal Muscle of mdx Mice*

We first studied the expression levels of various MMPs and related genes in skeletal muscle of *mdx* mice using a PCR gene array technique (SABiosciences, Frederick, MD) that examined the mRNA levels of 89 genes. Analyses of PCR arrays revealed that mRNA levels of several MMPs (eg, MMP-3, -8, -9, -10, -12, -13, -14, and -15) were increased, although MMP-11 showed down-regulation in gastrocnemius muscle of *mdx* mice in comparison with control mice (Table 1). The expression of a disintegrin and metallopeptidase (reprolysin type) with thrombospondin type 1 motif (Adamts) proteases, which are also involved in remodeling processes, was also found to be differentially regulated. Whereas the expression of Adamts1, Adamts5, and Adamts8 were reduced, the transcript level of Adamts2 was increased in gastrocnemius muscle of *mdx* mice compared with control mice (Table 1). Out of four known physiological inhibitors of MMPs (TIMPs), mRNA levels of TIMP-2 and TIMP-3 were reduced and the expression of TIMP-1 was enhanced in *mdx* mice compared with control mice. Furthermore, the mRNA levels of several cell adhesion molecules (eg, NCAM1, NCAM2, ICAM1, VCAM1, and L-selectin/Sel1) and connective tissue growth factor (Ctgf) were increased in gastrocnemius muscle of *mdx* mice compared with controls. The expression of several collagen genes (eg, Col1a1, Col3a1, Col4a1, Col4a2, and Col5a1) was increased in gastrocnemius muscle of *mdx* mice (Table 1). In contrast, the expression of Col2a1 and Col4a3

**Table 1.** Fold Changes in mRNA Levels of Various MMPs and Related Genes in Gastrocnemius Muscle of 6-Week-Old *mdx* Mice Compared to Control Mice Determined by PCR Gene Array Technique

Gene symbol	GenBank accession no.	Fold change
<i>Adamts1</i>	NM_009621	-2.6
<i>Adamts2</i>	NM_175643	1.72
<i>Adamts5</i>	NM_011782	-1.43
<i>Adamts8</i>	NM_013906	-1.31
<i>Col1a1</i>	NM_007742	3.37
<i>Col2a1</i>	NM_031163	-1.28
<i>Col3a1</i>	NM_009930	2.75
<i>Col4a1</i>	NM_009931	1.53
<i>Col4a2</i>	NM_009932	1.18
<i>Col4a3</i>	NM_007734	-1.82
<i>Col5a1</i>	NM_015734	1.26
<i>Ctgf</i>	NM_10217	1.34
<i>Ncam1</i>	NM_010875	1.53
<i>Ncam2</i>	NM_010954	1.59
<i>Icam1</i>	NM_010493	1.22
<i>Vcam1</i>	NM_011693	2.89
<i>Sell</i>	NM_011346	1.45
<i>Mmp3</i>	NM_010809	1.91
<i>Mmp8</i>	NM_008611	1.11
<i>Mmp9</i>	NM_013599	2.78
<i>Mmp10</i>	NM_019471	1.16
<i>Mmp11</i>	NM_008606	-1.41
<i>Mmp12</i>	NM_008605	1.33
<i>Mmp13</i>	NM_008607	1.41
<i>Mmp14</i>	NM_008608	2.76
<i>Mmp15</i>	NM_008609	1.11
<i>Timp1</i>	NM_011593	3.1
<i>Timp2</i>	NM_011594	-1.54
<i>Timp3</i>	NM_011595	-2.02

diminished in dystrophic muscle of *mdx* mice compared with controls (Table 1).

To validate the results of PCR array experiment, we performed QRT-PCR for a few MMP-related genes on gastrocnemius muscle of individual control and *mdx* mice. As shown in Figure 1A, QRT-PCR results showed good correlation with PCR array experiment. The transcript levels of MMP-3, MMP-10, MMP-14, VCAM-1, Col1a1, and Col3a1 were significantly higher, whereas the mRNA levels of TIMP-2 were significantly lower in *mdx* mice compared with control mice (Figure 1A). We next sought to determine whether enzymatic activity of MMPs was also similarly increased in skeletal muscle of *mdx* mice. To determine the activities of MMPs, we used a commercially available fluorescence-based MMPs assay kit (AnaSpec, Fremont, CA). The kit measures the activities of a variety of MMPs including MMP-1, -2, -7, -8, -9, -10, -13, and -14. Consistent with the increased expressions of several MMPs, the enzymatic activities of MMPs were also found to be significantly higher in gastrocnemius muscle of *mdx* mice compared with the age-matched control mice (Figure 1B). Similar increased expressions and activities of MMPs were also observed in tibial anterior muscle of *mdx* mice (data not shown). Taken together, these results provide strong evidence that the expressions and activities of MMPs are dysregulated in dystrophic muscle of *mdx* mice.

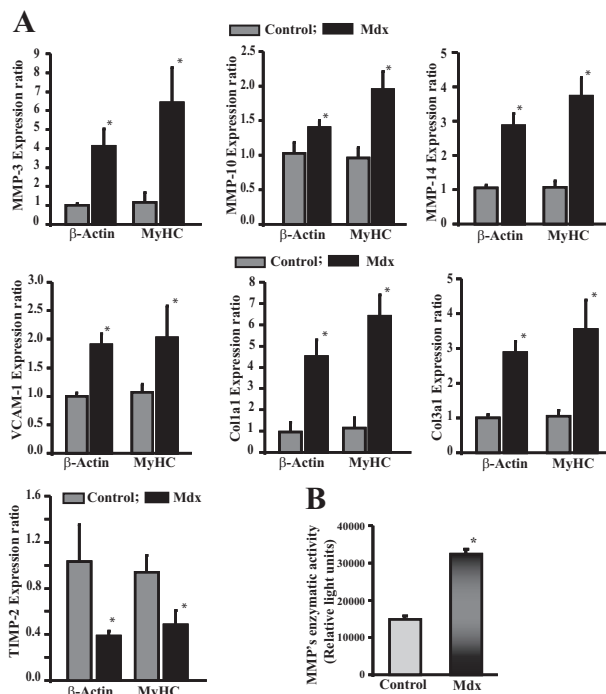


**Figure 1.** Increased expression of MMPs, cell adhesion molecules, and collagens in skeletal muscle of *mdx* mice. **A:** Gastrocnemius muscle from 6-week-old control and *mdx* mice were isolated and used to study the mRNA levels of MMP-3, MMP-10, MMP-14, VCAM-1, Col1a1, Col3a1, and TIMP-2. Data presented here show that the mRNA levels of MMP-3, MMP-10, MMP-14, VCAM-1, Col1a1, and Col3a1 were significantly increased, whereas mRNA levels of TIMP-2 were significantly reduced in gastrocnemius muscle of *mdx* mice ( $N = 4$ ) compared with control mice ( $N = 4$ ). The mRNA levels were normalized using  $\beta$ -actin and MyHC as housekeeping genes. **B:** Data presented here show that the enzymatic activity of MMPs is significantly increased in gastrocnemius muscle of *mdx* mice compared with control mice. \* $P < 0.01$ , values significantly different from wild-type mice.

### Batimastat Improves Skeletal Muscle Structure and Reduces Fibrosis in *mdx* Mice

Control and *mdx* mice were given chronic administration of batimastat, a broad spectrum inhibitor of MMPs 22-24 or vehicle alone for a total of 5 weeks followed by isolation of skeletal muscle and performing H&E staining. As shown in Figure 2A (top), there was no apparent difference in skeletal muscle structure of control mice treated with vehicle or batimastat. Skeletal muscle of *mdx* mice treated with vehicle alone showed typical features of muscular dystrophy including the fibers of variable sizes, central nucleation, increased area under necrosis, and cellular infiltrates within muscle cross-sections (Figure 2A). However, the variability in fiber cross-sectional area, the extent of degeneration/regeneration, and cellular infiltrates seems to be reduced in quadriceps and diaphragm on treatment of *mdx* mice with batimastat (Figure 2, A and B). Similar improvement in muscle structure was also observed in gastrocnemius and soleus muscles of batimastat-treated *mdx* mice (data not shown). Since repeated cycles of muscle degeneration and regeneration and inflammation leads to the development of interstitial fibrosis in skeletal muscle of *mdx* mice, we also determined whether treatment with batimastat can reduce level of fibrosis in dystrophic muscle *mdx* mice. Staining

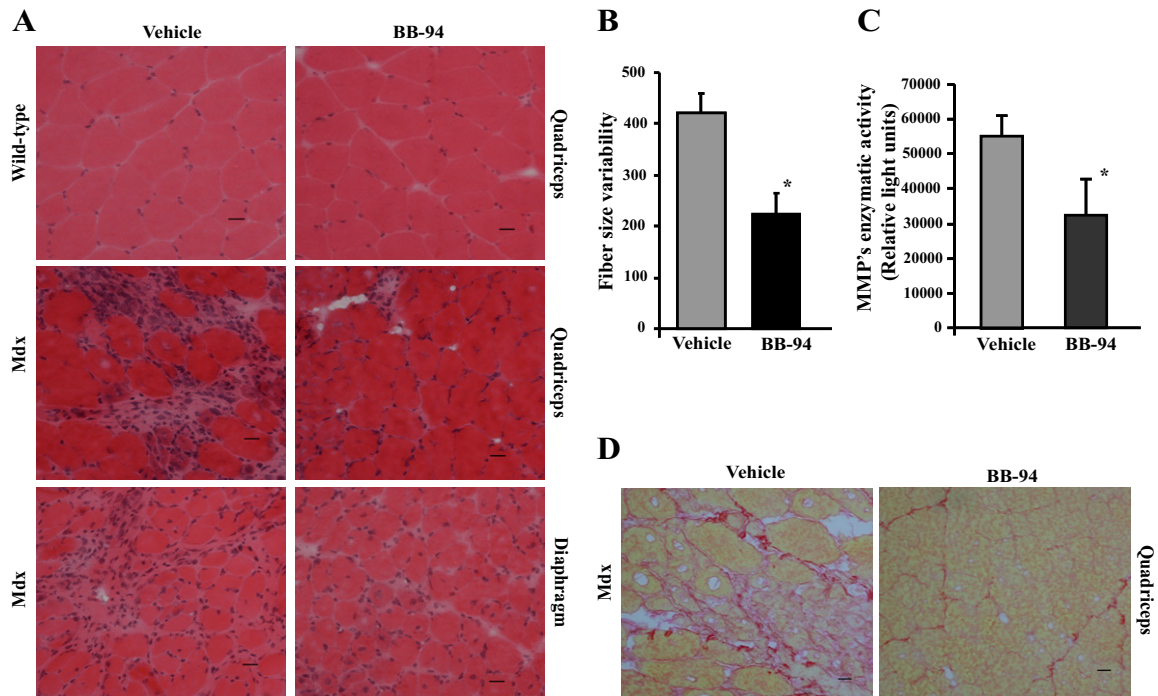


**Figure 2.** Effects of chronic administration of batimastat on skeletal muscle structure and fibrosis in *mdx* mice. Starting at the age of two weeks, control and *mdx* were given chronic administration of batimastat (BB-94) or vehicle alone for a total of five weeks as described in *Materials and Methods*. **A:** H&E staining of muscle sections showed that batimastat did not affect skeletal muscle structure in control mice (**top**). Treatment with batimastat significantly improved muscle structure in quadriceps (**middle**) and diaphragm (**bottom**) of *mdx* mice. **B:** Histogram shows variability in fiber diameter of diaphragm in *mdx* mice treated with vehicle or BB-94. The data represent the mean of the SD of fibers. \* $P < 0.01$ , values significantly different from vehicle alone-treated *mdx* mice,  $N = 6$  in each group. Scale bar = 20  $\mu\text{m}$ . **C:** Data presented here show that the enzymatic activity of MMPs is significantly reduced in gastrocnemius muscle of BB-94-treated *mdx* mice compared with vehicle alone treated *mdx* mice. \* $P < 0.05$ , values significantly different from wild-type mice ( $N = 4$  in each group). **D:** Representative Sirius red stained images show reduced fibrosis in quadriceps muscle of BB-94-treated *mdx* mice compared with those treated with vehicle alone. Scale bar = 20  $\mu\text{m}$ .

of quadriceps muscle sections with Sirius red dye (which stains collagens) revealed considerably reduced fibrosis in batimastat treated *mdx* mice compared with control mice (Figure 2D). Finally, we also confirmed that treatment of *mdx* mice with batimastat significantly reduced the enzymatic activity of MMPs in skeletal muscle of *mdx* mice (Figure 2C). These data provide the initial evidence that the inhibition of MMPs using batimastat reduces skeletal muscle structural abnormalities and fibrosis in *mdx* mice.

### Batimastat Reduces the Accumulation of Macrophages and the Expression of Inflammatory Molecules in Skeletal Muscle of *mdx* Mice

Inflammation is a major pathological feature that contributes significantly to the disease progression and fiber necrosis in muscular dystrophy.<sup>38–41</sup> To understand whether increased levels of MMPs play a role in exacerbating inflammatory response in skeletal muscle of *mdx* mice, we studied the accumulation of macrophages in myofibers of vehicle and batimastat-treated *mdx* mice by immunostaining muscle sections with Mac-1 antibody. As shown in Figure 3A, treatment of *mdx* mice with batimastat reduced the concentration of macrophages in dystrophic muscles. To further confirm that batimastat decreases accumulation of macrophages in muscle tissues,

we also performed QRT-PCR to determine the mRNA levels of Mac-1 and CD68, the major cell surface markers for macrophages.<sup>20</sup> Consistent with immunohistological results, the mRNA levels of both Mac-1 and CD68 were found to be significantly reduced in gastrocnemius muscle of batimastat-treated *mdx* mice compared with control mice (Figure 3B) further suggesting that batimastat reduces the accretion of macrophages in dystrophic muscles of *mdx* mice.

Previously, reports have suggested that the expressions of various inflammatory cytokines, cell adhesion molecules, and collagens are increased in skeletal muscle of *mdx* mice.<sup>7,8,42,43</sup> By performing QRT-PCR, we studied the expressions of a few inflammatory molecules in skeletal muscle of *mdx* mice. As shown in Figure 3C, the mRNA levels of tumor necrosis factor (TNF)- $\alpha$ , intracellular cell adhesion molecule-1 (ICAM-1), and vascular cell adhesion molecule-1 (VCAM-1) were found to be significantly reduced in the skeletal muscle of batimastat-treated *mdx* mice compared with vehicle alone-treated *mdx* mice. Collagen I and collagen III are the major collagens present in extracellular matrix of skeletal muscle and their levels are increased in dystrophic muscle of *mdx* mice.<sup>20,44</sup> Although the level of collagen I (ie, Col1a1) was not affected, the mRNA level of collagen III (ie, Col3a1) was found to be significantly reduced on treatment of *mdx* mice with batimastat (Figure 3C).

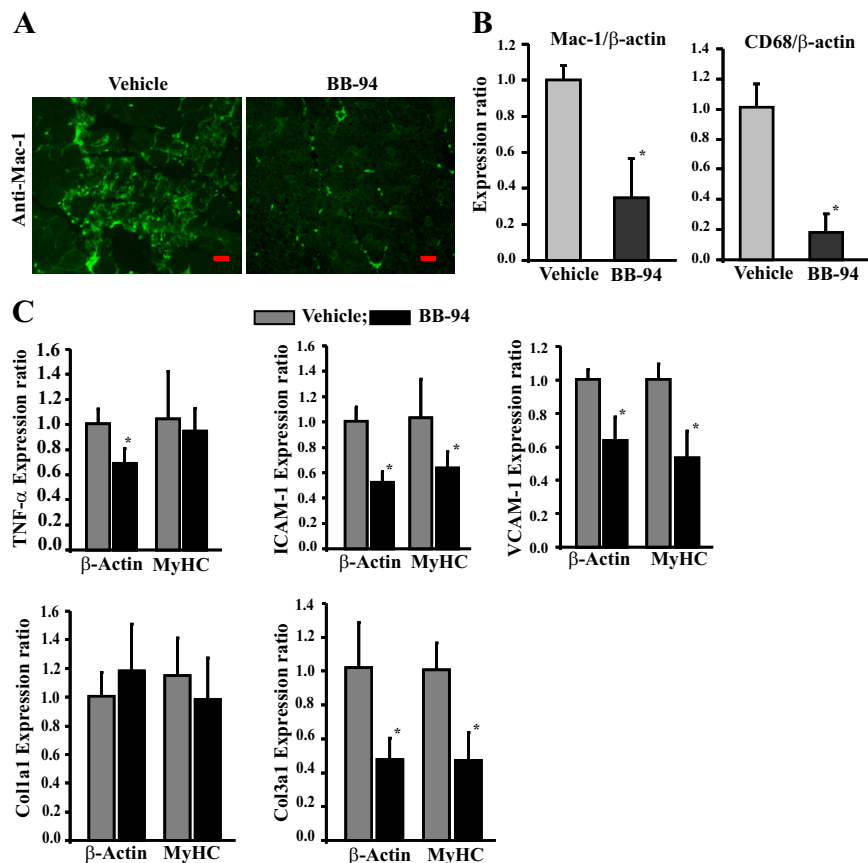


**Figure 3.** Effects of batimastat on the accumulation of macrophages and expression of inflammatory molecules in skeletal muscle of *mdx* mice. **A:** Gastrocnemius muscle sections of vehicle or batimastat (BB-94)-treated *mdx* mice were stained with Mac-1 antibody. Representative photomicrographs presented here show that batimastat reduced the concentration of macrophages in *mdx* mice.  $N = 6$  in each group. Scale bar = 20  $\mu$ m. **B:** QRT-PCR analysis (normalized to  $\beta$ -actin) showed a significant reduction in the mRNA levels of macrophage markers Mac-1 and CD68 in gastrocnemius muscle of batimastat-treated *mdx* ( $N = 4$ ) mice compared with vehicle alone-treated *mdx* ( $N = 4$ ) mice. **C:** Transcript levels of TNF- $\alpha$ , ICAM-1, VCAM-1, and Col3a1 but not Col1a1 were also found to be significantly reduced in gastrocnemius muscle of batimastat-treated *mdx* mice ( $N = 4$ ) compared with *mdx* mice given vehicle alone ( $N = 4$ ). The mRNA levels were normalized using  $\beta$ -actin and MyHC as housekeeping genes. \* $P < 0.01$ , values significantly different from vehicle-alone treated *mdx* mice.

### Batimastat Reduces Fiber Necrosis and Increases the Protein Levels of nNOS and $\beta$ -Dystroglycan in Skeletal Muscle of *mdx* Mice

Dystrophin deficiency causes increased sarcolemmal permeability and fiber necrosis.<sup>20,45</sup> We next sought to determine whether the inhibition of MMPs using batimastat can improve sarcolemma integrity and reduce fiber necrosis in *mdx* mice. The permeable/necrotic fibers in gastrocnemius muscle of *mdx* mice were quantified by immunostaining the muscle sections with Cy3-labeled anti-mouse IgG. As shown in Figure 4A, the *mdx* mice treated with vehicle alone showed high intracellular staining for IgG within a part of their muscle fibers. However, the number of IgG-stained muscle fibers was significantly reduced in gastrocnemius muscle of *mdx* mice on treatment with batimastat (Figure 4, A and B).

Although the deficiency of dystrophin is the primary cause for DMD, it has been consistently observed that the loss of dystrophin perturbs the structural composition of DGC in such a way that the levels of almost all of the members of DGC and associated proteins are affected in skeletal muscle fibers.<sup>46,47</sup> It has also been reported that the levels of utrophin, a homologue of dystrophin, are increased in skeletal muscle of *mdx* mice, which may account for reduced pathogenesis in *mdx* mice compared with DMD patients.<sup>1,2,48,49</sup> We investigated whether the inhibition of MMPs modulates the levels of various DGC-related proteins. Interestingly, treatment with batimastat

significantly increased the levels of neuronal nitric oxide synthase (nNOS) and  $\beta$ -dystroglycan compared with those treated with vehicle alone. In contrast, there was no significant difference in levels of utrophin and  $\alpha$ -dystrobrevin protein in batimastat-treated and vehicle alone-treated *mdx* mice (Figure 4, C and D).

### Batimastat Reduces the Number of Centronucleated Fibers and the Expression of E-MyHC in Skeletal Muscle of *mdx* Mice

At the initial stages of disease progression, the necrotic fibers in skeletal muscle of DMD patients or animal models are replaced by new myofibers depicted by increased number of centrally nucleated fibers. These newly formed myofibers express E-MyHC and other markers such as myogenin. Since fiber necrosis was significantly reduced in batimastat-treated *mdx* mice, we next sought to determine the effects of batimastat on the formation of new myofibers in their skeletal muscle. Interestingly, the number of centronucleated fibers was significantly reduced in skeletal muscle of batimastat-treated gastrocnemius muscle compared with vehicle alone-treated *mdx* mice (Figure 5, A and B). Furthermore, number of E-MyHC-stained myofibers was also considerably reduced in gastrocnemius muscle of batimastat-treated *mdx* mice compared with those administered vehicle alone (Figure 5A), which was further confirmed by

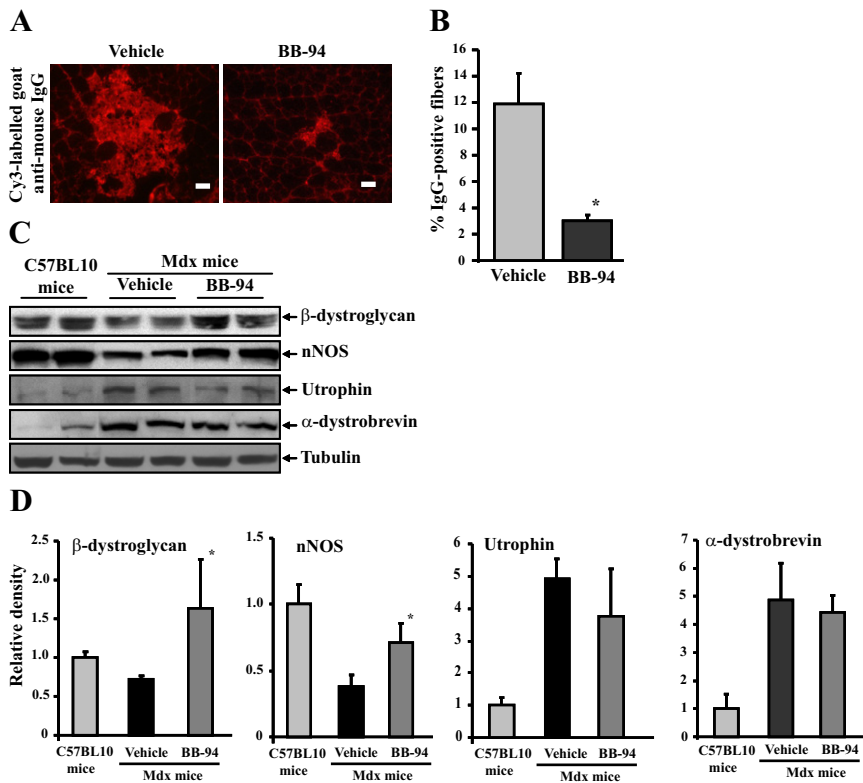


**Figure 4.** Effects of batimastat on sarcolemmal permeability and levels of cytoskeletal proteins in *mdx* mice. **A:** Gastrocnemius muscle cross-sections from vehicle alone or batimastat (BB-94)-treated *mdx* mice were immunostained with Cy3-labeled goat anti-mouse IgG to detect permeable/damaged fibers. **B:** Quantification of Cy3-positive fibers showed a significant reduction in number of IgG permeable fibers in gastrocnemius muscle of batimastat-treated *mdx* mice ( $N = 6$ ) compared with *mdx* mice treated with vehicle alone ( $N = 6$ ).  $*P < 0.05$ , values significantly different from *mdx* mice treated with vehicle alone. Scale bar = 20  $\mu\text{m}$ . **C:** Tissue extracts prepared from gastrocnemius muscle of control mice and untreated or batimastat-treated *mdx* mice were analyzed by Western blot. Representative immunoblots presented here show that the levels of  $\beta$ -dystroglycan and nNOS protein were considerably increased in batimastat-treated *mdx* mice compared with vehicle alone-treated *mdx* mice. The protein level of utrophin,  $\alpha$ -dystrobrevin and an unrelated protein tubulin remained unchanged. **D:** Quantification of Western blot (normalized with tubulin) showed a significant increase in protein levels of  $\beta$ -dystroglycan and nNOS but not utrophin or  $\alpha$ -dystrobrevin in BB-94-treated *mdx* mice compared with vehicle alone-treated *mdx* mice.  $*P < 0.01$ , values significantly different from vehicle alone-treated *mdx* mice.

performing Western blot using E-MyHC antibody (Figure 5C). Moreover, the transcript level of myogenin was also significantly lower in gastrocnemius muscle of batimastat-treated *mdx* mice compared with control mice (Figure 5D). The reduction in the number of centronucleated fibers and E-MyHC-positive myofibers is consistent with the reduced fiber degeneration and improvement in skeletal muscle structure in batimastat-treated *mdx* mice compared with those treated with vehicle alone.

### Batimastat Improves Skeletal Muscle Strength in *mdx* Mice

Since batimastat was effective in reducing several pathological features in *mdx* mice, we investigated the effects of batimastat on functional aspects of muscle by measuring force production in isometric contractions. We used diaphragm muscle from wild-type and batimastat-treated and corresponding vehicle alone-treated *mdx* mice for these studies. Diaphragm was stimulated at different frequencies and absolute and specific muscle force produced in isometric contractions was measured. In agreement with reduced pathology in batimastat-treated *mdx* mice, diaphragm force production was significantly higher in batimastat-treated *mdx* mice compared with vehicle alone-treated mice (Figure 6, A and B). The diaphragm muscle weight per unit area was also significantly reduced in batimastat-treated *mdx* mice compared with those treated with vehicle alone (Figure 6C) further indicating the reduction in muscle hypertrophy and pathology in batimastat-treated *mdx* mice.

### Batimastat Inhibits the Activation of Extracellular-Regulated Kinase 1/2 (ERK1/2), p38 Mitogen-Activated Protein Kinase (MAPK), and Activator Protein-1 (AP-1) in Skeletal Muscle of *mdx* Mice

We have previously reported that the activation of ERK1/2 and AP-1 is significantly increased in skeletal muscle of *mdx* mice.<sup>4</sup> Published reports also suggest increased activation of other MAPKs (eg, JNK1 and p38) at different stages of disease progression in skeletal muscle of *mdx* mice.<sup>50–53</sup> Furthermore, it has been found that the activation of MAPKs cause the pathogenesis not only in dystrophin-deficient myofibers but also in several other types of muscular dystrophies.<sup>6</sup> We investigated whether treatment with batimastat affects the activation of these signaling proteins in skeletal muscle of *mdx* mice. Consistent with previously published reports,<sup>4,50</sup> a significant increase in the levels of phosphorylated ERK1/2 and p38 MAPK was observed in gastrocnemius muscle of *mdx* mice compared with control mice (Figure 7A). Interestingly, treatment of *mdx* mice with batimastat reduced in the activation of both ERK1/2 and p38MAPK in gastrocnemius muscle (Figure 7A). However, we did not find any significant difference in the levels of phosphorylated JNK1 in gastrocnemius muscle of *mdx* mice compared with control mice. Furthermore, batimastat did not affect the levels of JNK in gastrocnemius muscle of *mdx* mice (Figure 7A).

The activation of MAPK generally leads to the downstream activation of various nuclear transcription factors,

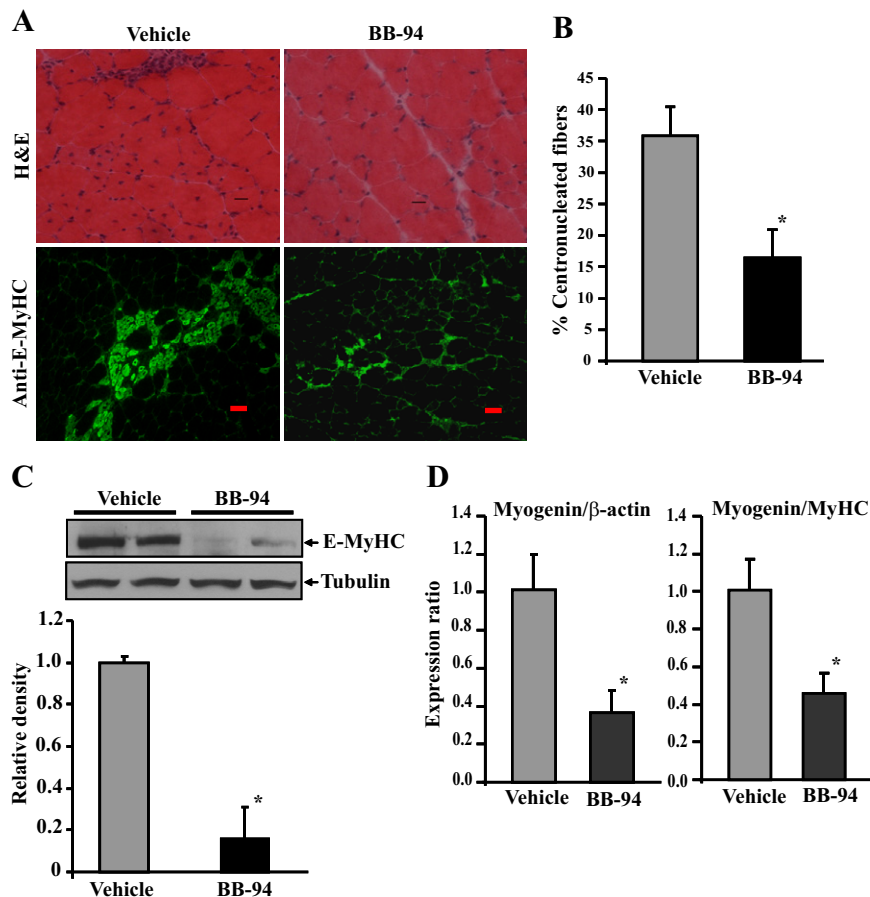


**Figure 5.** Effects of batimastat on number of centronucleated fibers and E-MyHC fibers in skeletal muscle of *mdx* mice. **A:** Gastrocnemius muscle sections of vehicle or batimastat (BB-94)-treated *mdx* mice were stained with H&E or embryonic/developmental myosin heavy chain antibody. Representative photomicrographs presented here show that number of centronucleated and anti-EMyHC-stained fibers were considerable reduced in batimastat (BB-94)-treated *mdx* mice compared with vehicle alone-treated *mdx* mice. Scale bar = 20  $\mu$ m. **B:** Quantification of centronucleated fibers showed significantly reduced number in batimastat-treated *mdx* mice ( $N = 6$ ) compared with vehicle-alone treated *mdx* mice ( $N = 7$ ). \* $P < 0.05$ , values significantly different from vehicle alone-treated *mdx* mice. **C:** Representative immunoblots and quantification presented here show reduced levels of embryonic/developmental myosin heavy chain protein in gastrocnemius muscle of batimastat-treated *mdx* mice compared with vehicle alone-treated *mdx* mice. \* $P < 0.01$ , values significantly different from vehicle-treated *mdx* mice. **D:** The mRNA level of myogenin (normalized with  $\beta$ -actin or MyHC4) was significantly lower in gastrocnemius muscle of batimastat-treated *mdx* mice ( $N = 4$ ) compared with vehicle alone treated *mdx* mice ( $N = 4$ ). \* $P < 0.01$ , values significantly different from vehicle alone-treated *mdx* mice.

the most prominent being AP-1.<sup>54</sup> By performing electrophoretic mobility shift assay, we studied the effects of batimastat on the activation of AP-1 in skeletal muscle of *mdx* mice. The DNA-binding activity of AP-1 was considerably reduced in gastrocnemius muscle of batimastat-treated *mdx* mice compared with those treated with vehicle alone (Figure 7B).

### Discussion

Many pathological conditions including muscular dystrophy are distinguished by uncontrolled matrix degradation that results in excessive tissue destruction, disruption of matrix boundaries, and loss of extracellular matrix functions. MMPs play critical role in extracellular matrix turn-

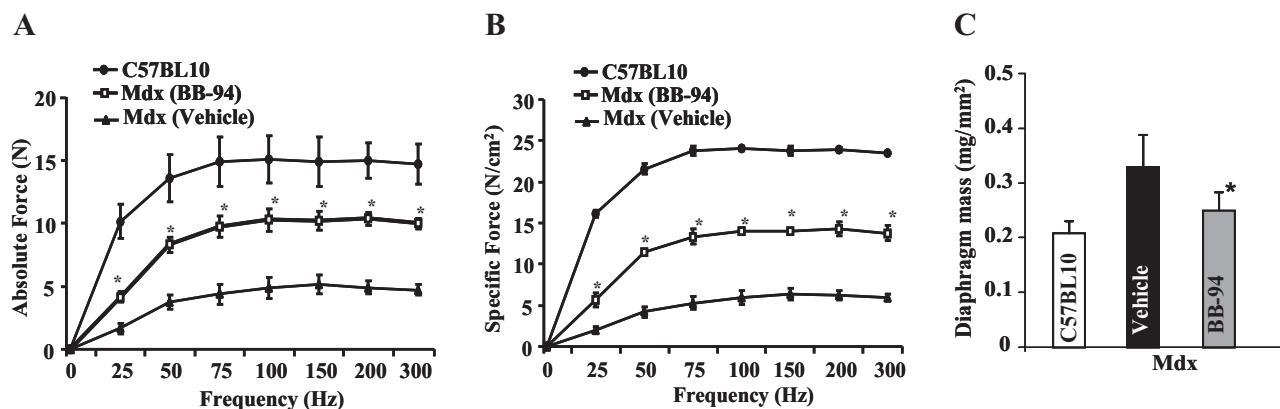


**Figure 6.** Effects of batimastat on muscle strength in *mdx* mice. Data presented here show that average (A) absolute force; and specific force (B) produced by diaphragm of batimastat-treated *mdx* mice was significantly higher as compared with *mdx* mice treated with vehicle alone. \* $P < 0.05$ , values significantly different from corresponding *mdx* mice treated with vehicle alone at corresponding frequency. **C:** Diaphragm muscle weight per unit area was also significantly reduced in BB-94-treated *mdx* mice compared with those treated with vehicle alone. \* $P < 0.05$ , values significantly different from vehicle alone-treated *mdx* mice.

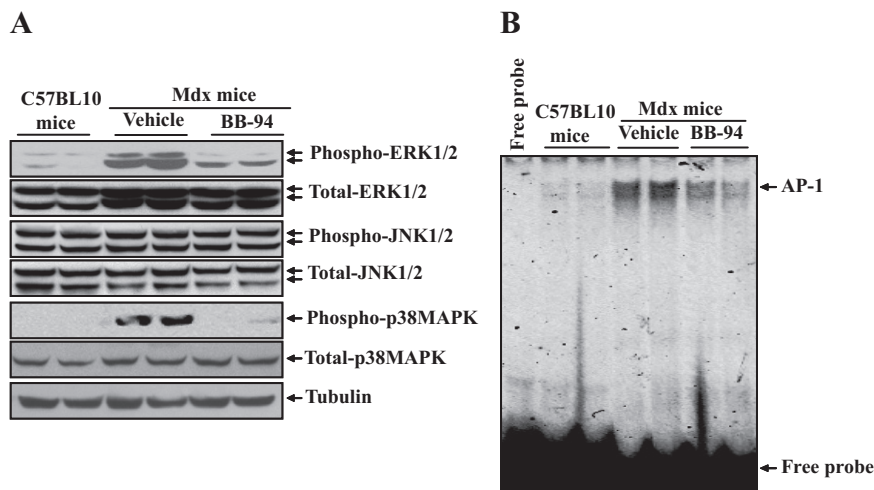


**Figure 7.** Effect of batimastat on the activation of MAPK and AP-1 in skeletal muscle of *mdx* mice. **A:** Gastrocnemius muscle from control, batimastat-treated, or untreated *mdx* mice were isolated and tissue extracts made were analyzed for the total and phosphorylated ERK1/2, JNK1/2, and p38 MAPK. Data presented here show that the levels of phosphorylated ERK1/2 and p38 MAPK were significantly reduced in batimastat-treated *mdx* mice compared with vehicle alone-treated *mdx* mice. **B:** Representative electrophoretic mobility shift assay gel presented here show that the DNA-binding activity of AP-1 was significantly reduced in gastrocnemius muscle of batimastat-treated *mdx* mice compared with *mdx* mice treated with vehicle alone.

over in physiological and pathological remodeling.<sup>11,18,19</sup> The excessive production of MMPs is also strongly linked with the initiation and perpetuation of inflammation and fibrosis in various diseases.<sup>11,13–17</sup> While muscular dystrophy involves considerable ECM abnormalities, the potential role of MMPs in the pathogenesis of muscular dystrophy is less well known.

In this study, we tested the hypothesis that broad inhibition of MMPs using pharmacological approaches will be effective in alleviating the pathology of *mdx* mice. Our results suggest that the expressions of a number of MMPs are significantly increased in dystrophic muscle of *mdx* mice (Table 1 and Figure 1). Our results also provide compelling evidence that broad spectrum MMP inhibitory drug batimastat, which has been used in several clinical trials in cancer patients,<sup>19,29–34</sup> ameliorates pathology of *mdx* mice. Although our study is a short-term where *mdx* mice were treated only for 5 weeks and further investigations are required involving long-term treatment protocols and higher animal models of DMD, it provides initial evidence that MMPs may serve as important molecular targets to alleviate the suffering of DMD patients.

Although the exact mechanisms by which increased levels of MMPs contribute to disease progression in *mdx* mice remain enigmatic, increased expression of MMPs in skeletal muscle microenvironment may cause the breakdown of the components of cytoskeleton-ECM network leading to sarcolemmal damage and fiber necrosis. Indeed, collagen IV (a major component of the basement membrane) and  $\beta$ -dystroglycan (an important protein of DGC) have already been validated as the direct targets of MMP-mediated proteolysis.<sup>11,12,55–57</sup> In addition, several other proteins such as laminin, fibronectin, entactin, and elastin present in ECM of skeletal muscle are also potential proteolytic targets of various MMPs.<sup>58–60</sup> Enhanced activity of MMPs may also cause the expression and/or proteolytic activation of various latent inflammatory cytokines, chemokines, and growth factors leading to inflammatory response and fibrosis in skeletal muscle.<sup>11</sup> Indeed, these postulations are well supported by our results that batimastat reduces the accumulation of macrophages in muscle tissues, bring about a reduction

in the expression of proinflammatory cytokine TNF- $\alpha$ , cell adhesion molecules (ICAM-1 and VCAM-1), and fibrosis-related gene Col3a1 (Figure 3), fiber necrosis (Figure 4), and improves overall muscle structure and function in *mdx* mice (Figures 2, 5, and 6).

We have also found that treatment with batimastat reduces sarcolemmal damage and fiber necrosis in skeletal muscle of *mdx* mice (Figure 4A). Although the lack of functional dystrophin is the primary cause for dystrophinopathy, the structural composition of the DGC and associated proteins is highly perturbed in skeletal muscle of DMD patients and *mdx* mice.<sup>46,47</sup> Our results demonstrate that batimastat significantly improves the levels of  $\beta$ -dystroglycan in skeletal muscle of *mdx* mice (Figure 4C), which is consistent with previously published reports that  $\beta$ -dystroglycan is proteolysed in MMP-dependent manner in dystrophic muscle of *mdx* mice.<sup>55,56</sup> Furthermore, the levels of nNOS, a protein that interacts with DGC in skeletal muscle, is reduced in dystrophic muscles of *mdx* mice and restoration of nNOS ameliorates muscle pathology in these mice.<sup>40</sup> It is interesting to note that nNOS is essential for maintenance of normal muscle activity *in vivo*<sup>61</sup> and genetic ablation of nNOS causes significant reduction in maximum tetanic force production and increases susceptibility to contraction-induced fatigue.<sup>62</sup> Since treatment of *mdx* mice with batimastat significantly enhanced protein levels of nNOS (Figure 4, C and D) and improved muscle force production in isometric contractions in diaphragm of *mdx* mice (Figure 6), elevated activity of MMPs may be one of potential reasons for the reduced levels of nNOS in dystrophic muscle of *mdx* mice. However, it remains unknown how MMPs affects the levels of nNOS in skeletal muscle of *mdx* mice. Though nNOS does not directly interact with  $\beta$ -dystroglycan in DGC (rather it interacts with  $\alpha$ -syntrophin), one of the possibilities could be that restoration of  $\beta$ -dystroglycan level on MMP inhibition improves the overall stability of DGC complex leading to increased expression of DGC-interacting proteins including nNOS in skeletal muscle. There is also a possibility that nNOS is directly proteolysed by MMPs due to accumulation of active MMPs in damaged/permeable myofibers of *mdx* mice.

Furthermore, a recent report from our laboratory also suggests that the protein (but not mRNA) levels of nNOS are significantly reduced by overexpression of inflammatory cytokine TNF-like weak inducer of apoptosis in skeletal muscle of mice.<sup>63</sup> Therefore, it is possible that the reduced levels of nNOS are a result of increased inflammation in skeletal muscle of *mdx* mice and batimastat augments nNOS protein levels by reducing inflammatory response in *mdx* mice as supported by our results in this study (Figure 3).

Another important finding of the present study was that batimastat reduced the number of centronucleated myofibers and fibers expressing E-MyHC suggesting that skeletal muscle regeneration is attenuated on general inhibition of MMPs in *mdx* mice. Since the treatment of *mdx* mice with batimastat prevented fiber necrosis (Figures 2A, 4A, and 4B), the reduced number of centrally nucleated myofibers and embryonic/developmental myosin heavy chain-positive fibers may be a result of considerable reduction in fiber necrosis/damage in batimastat-treated *mdx* mice eliminating the need for regeneration.

Accumulating evidence from our group and others suggests that lack of dystrophin leads to the activation of various proinflammatory signaling pathways and transcription factors (eg, MAPKs, AP-1 and NF- $\kappa$ B) leading to the increased levels of proinflammatory molecules.<sup>4,6–8,41,50</sup> Furthermore, the activation of proinflammatory signaling pathways also occurs in macrophages which infiltrate skeletal muscles of dystrophic animals.<sup>7</sup> Our experiments demonstrate that batimastat suppresses the activation of MAPK and their downstream phosphorylation target AP-1 in dystrophic muscle of *mdx* mice (Figure 7, A and B). Because several proinflammatory cytokines and cell adhesion molecules including TNF- $\alpha$ , ICAM-1, and VCAM-1 contain consensus AP-1 binding DNA sequences in their promoter/enhancer region,<sup>54</sup> the inhibition of AP-1 could also be one of the potential reasons for their reduced expression in skeletal muscle of batimastat-treated *mdx* mice.

Although our results suggest that batimastat is effective in reducing several pathological features in *mdx* mice, it is important to note that batimastat (and its analogue marimastat) and several other first generation broad spectrum MMP inhibitors failed in clinical trials mainly due to a musculoskeletal syndrome that reduced the overall quality of life for patients.<sup>18,64,65</sup> While there is no doubt that MMPs represent one of the most important therapeutic targets for tissue degenerative disorders, multiple reasons have been suggested for the failure of first generation MMP inhibitory drugs (including batimastat) in clinical trials. A current theory is that the majority of the side effects associated with MMP inhibitors in clinical trials are predominantly related to off-target metal (Zn and Fe) chelation from these drugs.<sup>66</sup> The strongest evidence for musculoskeletal syndrome side effects not being related to MMP inhibition per se comes from the use of drugs that do not cause metal chelation. A number of compounds have been reported to have the ability to block MMP activity or expression including bisphosphonates,<sup>67,68</sup> statins,<sup>69,70</sup> and antibiotics.<sup>71</sup> Of these, tetracycline-derivatives are the best studied with respect to MMP inhibition.<sup>72,73</sup> So far there is no evidence that treat-

ment with any of these drugs is associated with musculoskeletal syndrome, suggesting that new generation of better designed MMP inhibitors will be more effective in clinical trials.<sup>74</sup> Consistent with our findings, Girgenrath et al<sup>75</sup> have recently reported that the treatment with tetracycline derivatives doxycycline or minocycline improved postnatal growth, delayed the onset of hind-limb paralysis, and increased the life span of the laminin- $\alpha$ 2-null mice (a model of congenital muscular dystrophy) from approximately 32 days to 70 days. Similarly, doxycycline was effective in reducing the pathogenesis in a mouse model of oculopharyngeal muscular dystrophy<sup>76</sup> further indicating that the pharmacological inhibition of MMPs could be an important approach to enhance life span in muscular dystrophy patients.

Because some of the MMPs also play critical roles in various physiological processes, it is also important to take into consideration that global inhibition of MMPs for longer duration could lead to deleterious side effects. It may be more beneficial to target specific MMPs that are aberrantly regulated during disease progression. Though the development of such methods is still in infancy, targeting MMPs only in affected tissues may also avoid the associated side effects of inhibition of MMPs. Nevertheless, our present study demonstrating the efficacy of batimastat in reducing skeletal muscle pathology in *mdx* mice suggest that MMPs are potential drug targets for treatment of DMD patients. Certainly, more investigations are required to understand the effects of inhibition of MMPs by multiple approaches in animal models before considering MMPs as a therapeutic target for DMD patients.

## References

1. Emery AE: The muscular dystrophies. *Lancet* 2002, 359:687–695
2. Campbell KP: Three muscular dystrophies: loss of cytoskeleton-extracellular matrix linkage. *Cell* 1995, 80:675–679
3. Rando TA: The dystrophin-glycoprotein complex, cellular signaling, and the regulation of cell survival in the muscular dystrophies. *Muscle Nerve* 2001, 24:1575–1594
4. Kumar A, Khandelwal N, Malya R, Reid MB, Boriek AM: Loss of dystrophin causes aberrant mechanotransduction in skeletal muscle fibers. *FASEB J* 2004, 18:102–113
5. Stedman HH, Sweeney HL, Shrager JB, Maguire HC, Panettieri RA, Petrof B, Narusawa M, Lefterovich JM, Sladky JT, Kelly AM: The *mdx* mouse diaphragm reproduces the degenerative changes of Duchenne muscular dystrophy. *Nature* 1991, 352:536–539
6. Bhatnagar S, Kumar A: Therapeutic targeting of signaling pathways in muscular dystrophy. *J Mol Med* 2010, 88:155–166
7. Acharya S, Villalta SA, Bakkar N, Bupha-Intr T, Janssen PM, Carathers M, Li ZW, Beg AA, Ghosh S, Sahenk Z, Weinstein M, Gardner KL, Rafael-Fortney JA, Karin M, Tidball JG, Baldwin AS, Guttridge DC: Interplay of IKK/NF-kappaB signaling in macrophages and myofibers promotes muscle degeneration in Duchenne muscular dystrophy. *J Clin Invest* 2007, 117:889–901
8. Kumar A, Boriek AM: Mechanical stress activates the nuclear factor-kappaB pathway in skeletal muscle fibers: a possible role in Duchenne muscular dystrophy. *FASEB J* 2003, 17:386–396
9. Engvall E, Wewer UM: The new frontier in muscular dystrophy research: booster genes. *FASEB J* 2003, 17:1579–1584
10. Khurana TS, Davies KE: Pharmacological strategies for muscular dystrophy. *Nat Rev Drug Discov* 2003, 2:379–390
11. Page-McCaw A, Ewald AJ, Werb Z: Matrix metalloproteinases and

- the regulation of tissue remodelling. *Nat Rev Mol Cell Biol* 2007, 8:221–233
12. Vu TH, Werb Z: Matrix metalloproteinases: effectors of development and normal physiology. *Genes Dev* 2000, 14:2123–2133
  13. Chandler S, Miller KM, Clements JM, Lury J, Corkill D, Anthony DC, Adams SE, Gearing AJ: Matrix metalloproteinases, tumor necrosis factor and multiple sclerosis: an overview. *J Neuroimmunol* 1997, 72:155–161
  14. Hu J, Van den Steen PE, Sang QX, Opdenakker G: Matrix metalloproteinase inhibitors as therapy for inflammatory and vascular diseases. *Nat Rev Drug Discov* 2007, 6:480–498
  15. Waubant E, Goodkin DE, Gee L, Bacchetti P, Sloan R, Stewart T, Andersson PB, Stabler K, Miller K: Serum MMP-9 and TIMP-1 levels are related to MRI activity in relapsing multiple sclerosis. *Neurology* 1999, 53:1397–1401
  16. Hoyhtya M, Hujanen E, Turpeenniemi-Hujanen T, Thorgeirsson U, Liotta LA, Tryggvason K: Modulation of type-IV collagenase activity and invasive behavior of metastatic human melanoma (A2058) cells in vitro by monoclonal antibodies to type-IV collagenase. *Int J Cancer* 1990, 46:282–286
  17. Turpeenniemi-Hujanen T, Thorgeirsson UP, Hart IR, Grant SS, Liotta LA: Expression of collagenase IV (basement membrane collagenase) activity in murine tumor cell hybrids that differ in metastatic potential. *J Natl Cancer Inst* 1985, 75:99–103
  18. Fingleton B: Matrix metalloproteinases as valid clinical targets. *Curr Pharm Des* 2007, 13:333–346
  19. Fingleton B: MMPs as therapeutic targets—still a viable option?. *Semin Cell Dev Biol* 2008, 19:61–68
  20. Li H, Mittal A, Makonchuk DY, Bhatnagar S, Kumar A: Matrix metalloproteinase-9 inhibition ameliorates pathogenesis and improves skeletal muscle regeneration in muscular dystrophy. *Hum Mol Genet* 2009, 18:2584–2598
  21. Raffetto JD, Khalil RA: Matrix metalloproteinases and their inhibitors in vascular remodeling and vascular disease. *Biochem Pharmacol* 2008, 75:346–359
  22. Brown PD: Matrix metalloproteinase inhibitors: a novel class of anti-cancer agents. *Adv Enzyme Regul* 1995, 35:293–301
  23. Rasmussen HS, McCann PP: Matrix metalloproteinase inhibition as a novel anticancer strategy: a review with special focus on batimastat and marimastat. *Pharmacol Ther* 1997, 75:69–75
  24. Grams F, Crimmin M, Hinnes L, Huxley P, Pieper M, Tschesche H, Bode W: Structure determination and analysis of human neutrophil collagenase complexed with a hydroxamate inhibitor. *Biochemistry* 1995, 34:14012–14020
  25. Eccles SA, Box GM, Court WJ, Bone EA, Thomas W, Brown PD: Control of lymphatic and hematogenous metastasis of a rat mammary carcinoma by the matrix metalloproteinase inhibitor batimastat (BB-94). *Cancer Res* 1996, 56:2815–2822
  26. Lein M, Jung K, Le DK, Hasan T, Ortel B, Borchert D, Winkelmann B, Schnorr D, Loenings SA: Synthetic inhibitor of matrix metalloproteinases (batimastat) reduces prostate cancer growth in an orthotopic rat model. *Prostate* 2000, 43:77–82
  27. Low JA, Johnson MD, Bone EA, Dickson RB: The matrix metalloproteinase inhibitor batimastat (BB-94) retards human breast cancer solid tumor growth but not ascites formation in nude mice. *Clin Cancer Res* 1996, 2:1207–1214
  28. Watson SA, Morris TM, Robinson G, Crimmin MJ, Brown PD, Hardcastle JD: Inhibition of organ invasion by the matrix metalloproteinase inhibitor batimastat (BB-94) in two human colon carcinoma metastasis models. *Cancer Res* 1995, 55:3629–3633
  29. Bramhall SR, Hallissey MT, Whiting J, Scholefield J, Tierney G, Stuart RC, Hawkins RE, McCulloch P, Maughan T, Brown PD, Baillet M, Fielding JW: Marimastat as maintenance therapy for patients with advanced gastric cancer: a randomised trial. *Br J Cancer* 2002, 86:1864–1870
  30. Bramhall SR, Rosemurgy A, Brown PD, Bowry C, Buckels JA: Marimastat as first-line therapy for patients with unresectable pancreatic cancer: a randomized trial. *J Clin Oncol* 2001, 19:3447–3455
  31. Bramhall SR, Schulz J, Nemunaitis J, Brown PD, Baillet M, Buckels JA: A double-blind placebo-controlled, randomised study comparing gemcitabine and marimastat with gemcitabine and placebo as first line therapy in patients with advanced pancreatic cancer. *Br J Cancer* 2002, 87:161–167
  32. Macaulay VM, O'Byrne KJ, Saunders MP, Braybrooke JP, Long L, Gleeson F, Mason CS, Harris AL, Brown P, Talbot DC: Phase I study of intrapleural batimastat (BB-94), a matrix metalloproteinase inhibitor, in the treatment of malignant pleural effusions. *Clin Cancer Res* 1999, 5:513–520
  33. Nemunaitis J, Poole C, Primrose J, Rosemurgy A, Malfetano J, Brown P, Berrington A, Cornish A, Lynch K, Rasmussen H, Kerr D, Cox D, Millar A: Combined analysis of studies of the effects of the matrix metalloproteinase inhibitor marimastat on serum tumor markers in advanced cancer: selection of a biologically active and tolerable dose for longer-term studies. *Clin Cancer Res* 1998, 4:1101–1109
  34. Parsons SL, Watson SA, Steele RJ: Phase I/II trial of batimastat, a matrix metalloproteinase inhibitor, in patients with malignant ascites. *Eur J Surg Oncol* 1997, 23:526–531
  35. Wang X, Fu X, Brown PD, Crimmin MJ, Hoffman RM: Matrix metalloproteinase inhibitor BB-94 (batimastat) inhibits human colon tumor growth and spread in a patient-like orthotopic model in nude mice. *Cancer Res* 1994, 54:4726–4728
  36. Srivastava AK, Qin X, Wedhas N, Arnush M, Linkhart TA, Chadwick RB, Kumar A: Tumor necrosis factor-alpha augments matrix metalloproteinase-9 production in skeletal muscle cells through the activation of transforming growth factor-beta-activated kinase 1 (TAK1)-dependent signaling pathway. *J Biol Chem* 2007, 282:35113–35124
  37. Dogra C, Changotra H, Mohan S, Kumar A: Tumor necrosis factor-like weak inducer of apoptosis inhibits skeletal myogenesis through sustained activation of nuclear factor-kappaB and degradation of MyoD protein. *J Biol Chem* 2006, 281:10327–10336
  38. Spencer MJ, Tidball JG: Do immune cells promote the pathology of dystrophin-deficient myopathies? *Neuromuscul Disord* 2001, 11:556–564
  39. Spencer MJ, Walsh CM, Dorshkind KA, Rodriguez EM, Tidball JG: Myonuclear apoptosis in dystrophic *mdx* muscle occurs by perforin-mediated cytotoxicity. *J Clin Invest* 1997, 99:2745–2751
  40. Wehling M, Spencer MJ, Tidball JG: A nitric oxide synthase transgene ameliorates muscular dystrophy in *mdx* mice. *J Cell Biol* 2001, 155:123–131
  41. Hnia K, Gayraud J, Hugon G, Ramonatox M, De La Porte S, Matecki S, Mornet D: L-arginine decreases inflammation and modulates the nuclear factor-kappaB/matrix metalloproteinase cascade in *mdx* muscle fibers. *Am J Pathol* 2008, 172:1509–1519
  42. Wehling-Henricks M, Lee JJ, Tidball JG: Prednisolone decreases cellular adhesion molecules required for inflammatory cell infiltration in dystrophin-deficient skeletal muscle. *Neuromuscul Disord* 2004, 14:483–490
  43. Porter JD, Khanna S, Kaminski HJ, Rao JS, Merriam AP, Richmonds CR, Leahy P, Li J, Guo W, Andrade FH: A chronic inflammatory response dominates the skeletal muscle molecular signature in dystrophin-deficient *mdx* mice. *Hum Mol Genet* 2002, 11:263–272
  44. Wehling-Henricks M, Sokolow S, Lee JJ, Myung KH, Villalta SA, Tidball JG: Major basic protein-1 promotes fibrosis of dystrophic muscle and attenuates the cellular immune response in muscular dystrophy. *Hum Mol Genet* 2008, 17:2280–2292
  45. Straub V, Rafael JA, Chamberlain JS, Campbell KP: Animal models for muscular dystrophy show different patterns of sarcolemmal disruption. *J Cell Biol* 1997, 139:375–385
  46. Ohlendieck K, Campbell KP: Dystrophin-associated proteins are greatly reduced in skeletal muscle from *mdx* mice. *J Cell Biol* 1991, 115:1685–1694
  47. Ohlendieck K, Matsumura K, Ionasescu VV, Towbin JA, Bosch EP, Weinstein SL, Sernett SW, Campbell KP: Duchenne muscular dystrophy: deficiency of dystrophin-associated proteins in the sarcolemma. *Neurology* 1993, 43:795–800
  48. Dalkilic I, Kunkel LM: Muscular dystrophies: genes to pathogenesis. *Curr Opin Genet Dev* 2003, 13:231–238
  49. Tinsley J, Deconinck N, Fisher R, Kahn D, Phelps S, Gillis JM, Davies K: Expression of full-length utrophin prevents muscular dystrophy in *mdx* mice. *Nat Med* 1998, 4:1441–1444
  50. Hnia K, Hugon G, Rivier F, Masmoudi A, Mercier J, Mornet D: Modulation of p38 mitogen-activated protein kinase cascade and metalloproteinase activity in diaphragm muscle in response to free radical scavenger administration in dystrophin-deficient *Mdx* mice. *Am J Pathol* 2007, 170:633–643
  51. Nakamura A, Yoshida K, Takeda S, Dohi N, Ikeda S: Progression of dystrophic features and activation of mitogen-activated protein ki-

- nases and calcineurin by physical exercise, in hearts of mdx mice. *FEBS Lett* 2002, 520:18–24
52. Nakamura A, Yoshida K, Ueda H, Takeda S, Ikeda S: Up-regulation of mitogen activated protein kinases in mdx skeletal muscle following chronic treadmill exercise. *Biochim Biophys Acta* 2005, 1740:326–331
  53. Kolodziejczyk SM, Walsh GS, Balazsi K, Seale P, Sandoz J, Hierlihy AM, Rudnicki MA, Chamberlain JS, Miller FD, Megeney LA: Activation of JNK1 contributes to dystrophic muscle pathogenesis. *Curr Biol* 2001, 11:1278–1282
  54. Karin M: The regulation of AP-1 activity by mitogen-activated protein kinases. *J Biol Chem* 1995, 270:16483–16486
  55. Matsumura K, Zhong D, Saito F, Arai K, Adachi K, Kawai H, Higuchi I, Nishino I, Shimizu T: Proteolysis of beta-dystroglycan in muscular diseases. *Neuromuscul Disord* 2005, 15:336–341
  56. Michaluk P, Kolodziej L, Mioduszezewska B, Wilczynski GM, Dzwonek J, Jaworski J, Gorecki DC, Ottersen OP, Kaczmarek L: Beta-dystroglycan as a target for MMP-9, in response to enhanced neuronal activity. *J Biol Chem* 2007, 282:16036–16041
  57. Zhong D, Saito F, Saito Y, Nakamura A, Shimizu T, Matsumura K: Characterization of the protease activity that cleaves the extracellular domain of beta-dystroglycan. *Biochem Biophys Res Commun* 2006, 345:867–871
  58. Chakraborti S, Mandal M, Das S, Mandal A, Chakraborti T: Regulation of matrix metalloproteinases: an overview. *Mol Cell Biochem* 2003, 253:269–285
  59. Das S, Mandal M, Chakraborti T, Mandal A, Chakraborti S: Structure and evolutionary aspects of matrix metalloproteinases: a brief overview. *Mol Cell Biochem* 2003, 253:31–40
  60. Lewis MP, Machell JR, Hunt NP, Sinanan AC, Tippett HL: The extracellular matrix of muscle—implications for manipulation of the craniofacial musculature. *Eur J Oral Sci* 2001, 109:209–221
  61. Kobayashi YM, Rader EP, Crawford RW, Iyengar NK, Thedens DR, Faulkner JA, Parikh SV, Weiss RM, Chamberlain JS, Moore SA, Campbell KP: Sarcolemma-localized nNOS is required to maintain activity after mild exercise. *Nature* 2008, 456:511–515
  62. Percival JM, Anderson KN, Gregorevic P, Chamberlain JS, Froehner SC: Functional deficits in nNOSmu-deficient skeletal muscle: myopathy in nNOS knockout mice. *PLoS ONE* 2008, 3:e3387
  63. Mittal A, Bhatnagar S, Kumar A, Lach-Trifilieff E, Wauters S, Li H, Makonchuk DY, Glass DJ, Kumar A: The TWEAK-Fn14 system is a critical regulator of denervation-induced skeletal muscle atrophy in mice. *J Cell Biol* 2010, 188:833–849
  64. Brown PD: Clinical studies with matrix metalloproteinase inhibitors. *APMIS* 1999, 107:174–180
  65. Dove A: MMP inhibitors: glimmers of hope amidst clinical failures. *Nat Med* 2002, 8:95
  66. Renkiewicz R, Qiu L, Lesch C, Sun X, Devalaraja R, Cody T, Kaldjian E, Welgus H, Baragi V: Broad-spectrum matrix metalloproteinase inhibitor marimastat-induced musculoskeletal side effects in rats. *Arthritis Rheum* 2003, 48:1742–1749
  67. Giraudo E, Inoue M, Hanahan D: An amino-bisphosphonate targets MMP-9-expressing macrophages and angiogenesis to impair cervical carcinogenesis. *J Clin Invest* 2004, 114:623–633
  68. Ferretti G, Fabi A, Carlini P, Papaldo P, Cordiali Fei P, Di Cosimo S, Salesi N, Giannarelli D, Alimonti A, Di Cocco B, D'Agosto G, Bordignon V, Trento E, Cognetti F: Zoledronic-acid-induced circulating level modifications of angiogenic factors, metalloproteinases and proinflammatory cytokines in metastatic breast cancer patients. *Oncology* 2005, 69:35–43
  69. Yasuda S, Miyazaki S, Kinoshita H, Nagaya N, Kanda M, Goto Y, Nonogi H: Enhanced cardiac production of matrix metalloproteinase-2 and -9 and its attenuation associated with pravastatin treatment in patients with acute myocardial infarction. *Clin Sci (Lond)* 2007, 112:43–49
  70. Wilson WR, Evans J, Bell PR, Thompson MM: HMG-CoA reductase inhibitors (statins) decrease MMP-3 and MMP-9 concentrations in abdominal aortic aneurysms. *Eur J Vasc Endovasc Surg* 2005, 30:259–262
  71. Acharya MR, Venitz J, Figg WD, Sparreboom A: Chemically modified tetracyclines as inhibitors of matrix metalloproteinases. *Drug Resist Updat* 2004, 7:195–208
  72. Saikali Z, Singh G: Doxycycline and other tetracyclines in the treatment of bone metastasis. *Anticancer Drugs* 2003, 14:773–778
  73. Golub LM, Lee HM, Ryan ME, Giannobile WV, Payne J, Sorsa T: Tetracyclines inhibit connective tissue breakdown by multiple non-antimicrobial mechanisms. *Adv Dent Res* 1998, 12:12–26
  74. Abramovici H, Hogan AB, Obagi C, Topham MK, Gee SH: Diacylglycerol kinase-zeta localization in skeletal muscle is regulated by phosphorylation and interaction with syntrophins. *Mol Biol Cell* 2003, 14:4499–4511
  75. Girgenrath M, Beermann ML, Vishnudas VK, Homma S, Miller JB: Pathology is alleviated by doxycycline in a laminin-alpha2-null model of congenital muscular dystrophy. *Ann Neurol* 2009, 65:47–56
  76. Davies JE, Wang L, Garcia-Oroz L, Cook LJ, Vacher C, O'Donovan DG, Rubinsztein DC: Doxycycline attenuates and delays toxicity of the oculopharyngeal muscular dystrophy mutation in transgenic mice. *Nat Med* 2005, 11:672–677